buildings

MDPI

Article

Long-Term Urban Epidemic and Disaster Resilience: The Planning and Assessment of a Comprehensive Underground Resilience Core

Tong Qiu [1,2,3], Xiangsheng Chen [1,2,3,*], Dong Su [1,2,3] and Xingtao Lin [1,2,3]

[1] College of Civil and Transportation Engineering, Shenzhen University, Shenzhen 518060, China; 1950471009@email.szu.edu.cn (T.Q.); sudong@szu.edu.cn (D.S.); xtlin@szu.edu.cn (X.L.)
[2] Shenzhen Key Laboratory of Green, Efficient and Intelligent Construction of Underground Metro Station, Shenzhen 518060, China
[3] Key Laboratory for Resilient Infrastructures of Coastal Cities (MOE), College of Civil and Transportation Engineering, Shenzhen University, Shenzhen 518060, China
* Correspondence: xschen@szu.edu.cn

Abstract: This study utilizes the enclosed and stable environment of underground space for long-term sustainable planning for urban epidemics and disasters. Owing to the COVID-19 epidemic, cities require long-term epidemic–disaster management. Therefore, this study proposed a strategy for integrating multiple functions to plan a comprehensive Underground Resilience Core (URC). A planning and assessment methods of URC were proposed. With this methodology, epidemic- and disaster- URCs were integrated to construct a comprehensive-URC in underground spaces. The results show: (1) Epidemic-resilient URCs adopting a joint progressive approach with designated hospitals can rapidly suppress an epidemic outbreak. (2) The regularity of the morphology of underground spaces determines the area of the URC. Bar-shaped underground spaces have the potential for planning disaster-URCs. (3) The URC planning efficiency ranking is as follows: Bar shapes lead overall, T shapes are second under seismic resilience, and Cross shapes are second under epidemic resilience. (4) The potential analysis of planning a comprehensive-URC in the underground parking in Chinese cities showed that the recovery time can be advanced from 29% to 39% and the comprehensive resilience can be improved by 37.63%. The results of this study can serve as sustainable urban planning strategies and assessment tools for long-term epidemic–disaster management.

Keywords: comprehensive underground resilience core; disaster resilience; epidemic resilience; long-term epidemic–disaster management; underground space environment; underground parking

check for updates

Citation: Qiu, T.; Chen, X.; Su, D.; Lin, X. Long-Term Urban Epidemic and Disaster Resilience: The Planning and Assessment of a Comprehensive Underground Resilience Core. *Buildings* **2023**, *13*, 1292. https://doi.org/10.3390/buildings13051292

Academic Editor: John Kamara

Received: 18 March 2023
Revised: 20 April 2023
Accepted: 13 May 2023
Published: 16 May 2023

1. Introduction

The COVID-19 epidemic has posed new challenges to urban development and planning. Globally, cities are facing epidemics that are spreading from a single region to surrounding, national, and transnational cities. Studies have reported that the present development trends are likely to trigger rapid and widespread transmission of epidemics [1]. Moreover, urban planning is closely related to long-term disaster management, especially for earthquakes [2]. The urban agglomeration effect has become significant due to the improvement in the capacity, speed, and extent of transportation networks [3]. However, even though urban agglomeration signifies high-level urban development, it makes most cities disaster-prone. Hence, a comprehensive resilience assessment of urban spaces is required to ensure safety [4]. Underground space environments exhibit natural disaster robustness, spatial isolation, and environmental stability. Hence, the underground space environment is pivotal to urban disaster management [5]. In this study, high-level utilization strategies of underground spaces for urban long-term epidemic–disaster management were proposed. Specifically, this study addressed the following requirements of the underground space environment: (1) intensive planning for epidemic–disaster control spaces; (2) planning of underground spaces for long-term city routine operation and epidemic–disaster control; (3) planning of urban resilient underground spaces. Therefore, a novel method of the comprehensive resilience of underground space planning was proposed for urban epidemic–disaster management.

Epidemic control requires redundant medical supplies and space reserves to suppress outbreaks [6]. Especially, epidemic treatment requires an isolated environment to prevent infection [7]. Currently, temporary isolation hospitals are built for COVID-19 control [8]. However, because of the site constraints and isolation requirements, it is difficult to build temporary isolation hospitals in high-density cities. Additionally, recent studies have reported that aboveground temporary isolation hospitals were exposed to various risk factors, which had a detrimental effect on patients and operations [9]. Accordingly, urban managers and researchers have suggested that the underground emergency hospitals to mitigate the above-mentioned drawbacks. Underground emergency hospitals possess geotechnical environments with excellent airtightness, which are naturally isolated from aboveground space [10]. Furthermore, underground emergency hospitals integrate medical treatment and routine operation. A typical example is Sammy Ofer Fortified Underground Emergency Hospital in Haifa, Israel [11]. The hospital is a 1500-spot three-floor underground parking space. It can be converted into a 2000-bed underground emergency hospital within 12 h. Similarly, the Netherlands and Italy developed underground emergency hospitals to cope with infectious diseases, disasters, and wars [12]. Generally, underground emergency hospitals have the following unique epidemic-control characteristics: (1) the medical space can avoid the spread of epidemic air to the aboveground space; (2) air circulation in underground emergency hospitals is not affected by the aboveground environment; (3) toxic gases are disposed, filtered, and discharged through an organized system to achieve active control [13]. Finally, the use of underground space noncontact logistics can address the urban traffic needs in an epidemic and reduce the risk of infection during transportation [14]. An innovative underground logistics system based on metro and unmanned technology exhibits efficient and noncontact characteristics [15]. Therefore, building urban underground spaces is an efficient strategy for cities to cope with epidemics.

Besides epidemic emergencies, cities (agglomerations) are exposed to seismic risks. Regarding seismic vulnerability, urban underground spaces are resilient entities and act as a shelter site for earthquakes [16]. To ensure that underground structures can be transformed into reliable earthquake shelters, researchers have conducted various studies on the seismic vulnerability of underground structures. Tsinidis [17] performed a diverse soil-structure numerical parametric study to reveal the rectangular structure's seismic response characteristics. Sayed, Kwon [18] used a simulation technique to analyze the Daikai Station collapse during the 1995 Kobe earthquake. Dong, Jing [19] adopted a collapse process simulation for the seismic design of a rectangular underground structure. Zhong, Shen [20] used nonlinear static pushover analysis to study the seismic vulnerability of the Daikai station. Presently, most studies on the seismic performance of underground structures focus on subway station structures. However, subway stations are insufficient for urban epidemic–disaster management and for realizing the potential of urban underground spaces. Therefore, it is necessary to study the seismic damage modes of multitype underground spaces for a comprehensive resilience assessment of underground spaces. In this study, the characteristics and efficiency of typical large underground spaces for epidemic–disaster management were analyzed using megaseism finite element analysis.

The disaster management planning of underground spaces is crucial for the routine operation and emergency management of cities. Following the COVID-19 epidemic, urban planning considering the possibility of sudden epidemics/disasters is required in cities [21]. Moreover, underground spaces require dual planning for routine and emergency functions [22]. Researchers have conducted extensive research on urban planning for disaster management. Li, Zhao [23] reported that emergency shelter planning based on time-varying needs can reduce construction costs and the average victim evacuation distance. Breçani and Dervishi [24] found that large underground bunker networks exhibit high-energy-saving characteristics. Kitamura, Inazu [25] developed an allocation method for refugees and evacuation routes. Ćurković, Svetina [26] illustrated that comprehensive disaster management has a significant effect on disaster mitigation by studying Croatia experiencing both COVID-19 and an earthquake in 2020. However, current shelter planning does not include underground space epidemic management. Therefore, comprehensive epidemic–disaster management for large underground spaces is an urgent requirement. Moreover, the seismic performance of large underground spaces should be considered for disaster resilience planning [27]. Therefore, this study proposed a multistate transformation framework based on comprehensive epidemic–disaster management. Utilizing the proposed framework, large underground spaces with epidemic–disaster resilience were proposed. This study proposed underground spaces to build a comprehensive underground resilience core (URC).

To address the demands of large spaces for long-term epidemic–disaster management, this study proposed a novel URC planning strategy for urban underground spaces. Furthermore, methods for comprehensive resilience assessment of URCs were proposed. The methods quantitatively assessed the urban disaster management resilience and provided an important reference for the construction of existing and future urban underground spaces. The results of this study can guide the comprehensive planning of routine operations and the epidemic–disaster management of urban underground structures.

2. Methodology

This study aims to investigate URC planning and assessment methods. First, URC planning was conducted and large underground space models (Cross, T, and Bar) were constructed for epidemic-resilience URC planning. Second, the disaster-URC planning was conducted considering typical megaseism disasters. The epidemic-URC and disaster -URC were integrated to form the comprehensive-URC. Third, the URC schemes were assessed with URC morphology indicators. The comprehensive resilience assessment of the URC was conducted using the 2019 Wuhan COVID-19 data and 1995 Kobe earthquake data. Finally, the comprehensive resilience potential of urban underground spaces in China was analyzed.

2.1. URC Planning

A strategy for URC planning in large urban underground spaces was proposed in this study. Comprehensive resilience was considered as three modules, as Stock, Increment, and Variable. Comprehensive resilience was achieved by Stock–Increment–Variable transformation (Figure 1). With Stock as the core, the space and function transformed to Increment and Variable to improve urban resilience. Through emergency transformation of Increment and the sustainable transformation of Variable, long-term urban disaster management can be achieved. The efficiency of fully utilizing urban spaces was studied by analyzing the layouts of the URC planning in large underground spaces. URCs have the following characteristics: they are resilient to urban disasters; they offer a large space for epidemic–disaster management; they have multiple functions that ensure routine and emergency operations. The function and space of URCs were planned for Stock–Increment–Variable transformation, including:

(1) The URC included the Stock module. Large spaces were planned to meet the needs of citizens, as well as ensure necessary lifeline space and emergency transformation. Therefore, Stock should exhibit strong robustness.
(2) The URC included the Increment module for short-term disaster factors. Module Increment was multistate. When the disaster resistance demand exceeded the capacity of Stock, the Increment module provided a resilient reinforcement through an emergency transformation. Increment transformed into functions such as civil defense and epidemic–disaster control to accommodate citizens and absorb near-term uncertainty. Therefore, Increment should be resourceful, redundant, and inclusive.

(3) The URC included the Variable module to upgrade future resilience. Considering future developments and external uncertainty, Variable provided spaces that can be easily renovated and upgraded. Therefore, Variable should be reflective and flexible.

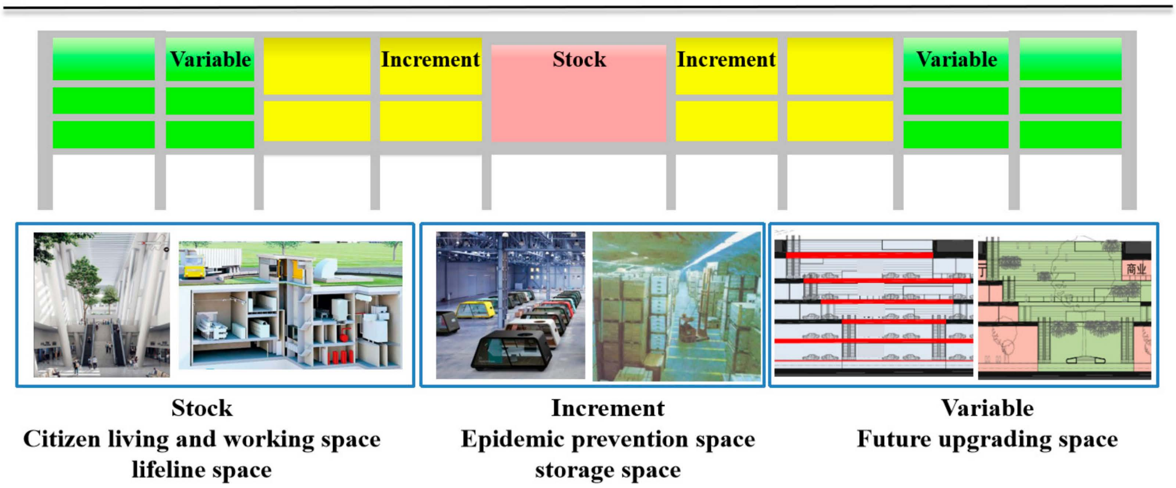

Figure 1. URC planning of Stock–Increment–Variable transformation.

To achieve comprehensive resilience, the URC integrated the functions and space of epidemic–disaster control. The URC planning methods are as follows:

(1) A large space with flexible functions was planned as Stock + Increment, and the outer areas were planned as Variable. Stock + Increment was planned as the epidemic URC.
(2) Stock was planned to deal with disasters. The underground disaster-resilience area was designated as Stock and the disaster-URC.
(3) Stock was planned by considering megaseism. The megaseism FEA was performed on the underground structures. The megaseism FEA revealed the damage modes of the large underground spaces. A safe distance was set to prevent uncertainty in linkage damage. A fixed distance between the first breakage and the URC was used as the safe distance to avoid an impact on the escape route. Stock was planned by combining the megaseism resilience area with the safety distance, which was also used in the disaster-URC.
(4) The disaster-URC and epidemic-URC were integrated, and Stock–Increment–Variable planning was conducted to construct the comprehensive URC.
(5) Comprehensive resilience was achieved by Stock–Increment–Variable transformation.

In general, underground large spaces with flexible functions were planned as the epidemic-URC, and each disaster-URC was planned through disaster analysis. Finally, the epidemic-URC and disaster-URC were integrated to form a comprehensive-URC with routine functions and disaster resilience.

2.2. URC Assessment

2.2.1. URC Morphology Assessment

The layout and size of the URC are closely related to the Stock–Increment–Variable transformation efficiency. Considering the requirements for comprehensive resilience, the URC should have the characteristics of inclusiveness, compactness, and regularity. Therefore, URC morphology indicators were established for the URC performance assessment. First, large spaces are not only required for routine operations but also for accommodating more citizens and ensuring flexible development. Therefore, a large underground space for URC planning can ensure strong resilience. D1 of Equation (1) was set based on the above characteristics. Furthermore, compactness is a key factor in the URC space layout. Compactness refers to a URC that is concentrated rather than spread out. A resilient URC should be centrally located and have a single strong resilient escape route to shorten the escape time. D2 of Equation (2) was set based on the above characteristics. Finally, regularity is a key factor in the layout of a URC space. The regularity refers to a regular geometry of the URC rather than having too many extending blocks. D3 of Equation (3) was set based on the above characteristics.

$$\mathrm{D1} = \frac{A_{\mathrm{S}}}{A_{\mathrm{S+I}}}, \frac{A_{\mathrm{S+I}}}{A_{\mathrm{S+I+V}}} \tag{1}$$

$$\mathrm{D2} = \frac{A_{\mathrm{Smax}}}{A_{\mathrm{S}}}, \frac{A_{\mathrm{S+Imax}}}{A_{\mathrm{S+I}}} \tag{2}$$

$$\mathrm{D3} = 2\sqrt{\pi\frac{A_{\mathrm{S}}}{L_{\mathrm{S}}}}, 2\sqrt{\pi\frac{A_{\mathrm{S+I}}}{L_{\mathrm{S+I}}}} \tag{3}$$

2.2.2. URC Comprehensive Resilience Assessment

This study used epidemic and megaseism time–history data for the comprehensive resilience assessment. Two datasets were used as the URC activation scenarios: (1) The 2019 Wuhan COVID-19 outbreak. Human-to-human transmission occurred during the epidemic. Approximately 50,000 people were eventually diagnosed with the infection [28]. (2) The 1995 Kobe earthquake in Japan occurred in Kansai, Japan. The earthquake had a magnitude of 7.3 on the Richter scale. Kobe is an important city in Kansai with a dense population. Approximately 300,000 people were affected and 43,792 people were injured [29]. These two typical urban emergency cases are typical to evaluate the comprehensive resilience of URCs.

The resilience functions were constructed for the URC assessment. The primary function of a URC is to provide a large space to accommodate the affected citizens. Therefore, its performance can be quantified by the number of cured citizens and bed supply. The process of establishing the resilience function was as follows. (1) The bed supply quantity was calculated based on the bed density of temporary isolation hospitals (Equation (4)). (2) Considering the epidemic–disaster difference, the bed demand was counted based on the time–history data (Equation (5)). The number of cured citizens was assumed to be proportional to the bed supply quantity, and the treatment capacity remains the same for each disaster. (3) The cure performance function Q_{c} was defined as the ratio of the performance recovery to the performance loss [30]. The difference between the current and maximum bed demands was used to characterize the performance recovery; the most critical maximum bed demand was used to characterize the performance loss (Equation (6)). The bed supply performance function Q_{b} was defined as the ratio of the current bed supply to the maximum bed supply (Equation (7)). Q_{b} and Q_{c} represent the process and outcome of performance, respectively. A comparative analysis of the two reveals the effect of bed supply on recovery. (4) $Q_{\mathrm{c}} - T$, $Q_{\mathrm{Bar}} - T$ functions and curves were established using the two time–history scenario data. (5) The $Q - T$ functions were integrated to obtain the resilience functions R_{e} and R_{s} (Equation (8)). The comprehensive resilience function R_{c} was superimposed on the two scenarios R (Equation (9)).

$$B_c = \rho A \tag{4}$$

$$B_{\mathrm{c}}(t) = \begin{cases} B_{\mathrm{R}} + B_{\mathrm{S}} - B_{\mathrm{C}} - B_{\mathrm{D}} \ldots \text{Epidemic} \\ B_{\mathrm{R}} - B_{\mathrm{C}} - B_{\mathrm{D}} \ldots\ldots\ldots\ldots \text{Disaster} \end{cases} \tag{5}$$

B_{R} represents bed demand, B_{S} represents bed demand of suspected cases, B_{C} represents the number of cured citizens, B_{D} represents the number of deaths, and ρ is 5.07 (m^2/bed) [31].

$$Q_{\mathrm{c}}(t) = \frac{B_{\mathrm{cMax}} - B_{\mathrm{c}}(t)}{B_{\mathrm{cMax}}} \tag{6}$$

$$Q_{\mathrm{b}}(t) = \frac{B_{\mathrm{b}}(t)}{B_{\mathrm{bMax}}} \tag{7}$$

$$R = \frac{\int_{t_0}^{t_{\max}} Q(t)dt}{(t_{\max} - t_0)Q(0)} \tag{8}$$

$$R_{\mathrm{c}} = R_{\mathrm{e}} + R_{\mathrm{s}} \tag{9}$$

where $Q(t)$ is the Q_{C} over time; t_0 and $t_{\max}$ are the time when the disaster starts and the maximum recovery time of multiple schemes, respectively; B_{cMax} indicates the maximum number of cured citizens; $B_{\mathrm{C(T)}}$ indicates the number of cured citizens at time t; $B_{\mathrm{b}}(t)$ indicates the bed supply at time t; B_{bMax} indicates the maximum quantity of the bed supply.

3. URC Planning Based on Typical Large Underground Spaces

Based on the URC planning, large spaces were used as Stock + Increment and the epidemic-URC. Subsequently, the disaster-URC planning was conducted considering multiple urban disasters. Focusing on urban megaseisms, the efficiency of the disaster-URC was analyzed. Finally, the functions and spaces of the epidemic- and disaster-URCs were integrated to build the comprehensive-URC.

3.1. Epidemic-URC

Typical large underground space schemes were selected to analyze the characteristics and efficiency of the URC planning. Typical large underground spaces include public buildings, commercial complexes, and subway hubs. A typical large underground space is a multifloor frame structure. A large underground space is merged with the surrounding and can be classified into "Cross", "T", and "Block" based on the morphology. The Cross(T)-shaped underground hub extending blocks tend to be functionally fixed and can be renovated and upgraded according to future demand. The central regions are set as lobbies with large spaces and high headroom, which are suitable for the Stock–Increment transformation. Bar-shaped underground spaces typically include large parking spaces. The spaces can be used as services and upgrades in the future. Therefore, most of the Bar-shaped large spaces are flexible.

Based on the above schemes, the epidemic-URC planning of typical large underground spaces was performed. Cross(T)-shaped underground hubs have complex functions. The extending blocks normally have insufficient space and fixed functions for emergency transformation. Flexible large spaces are arranged compactly and centrally, usually at the center of the block intersection. In contrast, the Bar shape is largely free of functional and spatial constraints, and Increment and Variable could be transformed in the short- and long-term according to demand, forming Stock + Increment (Variable). Note that the efficiency of the epidemic-URC is closely related to the URC area, and its capacity determines the bed supply capacity [32]. Therefore, except for Variable, large spaces with flexible functions in typical underground spaces were used for Stock + Increment and the epidemic-URC.

The start-up conditions for the epidemic-URCs were determined based on the COVID-19 epidemic control data. A mechanism for the rapid transformation between routine and epidemic states needs to be established with the following requirements: (1) long-term adequate reserves of medical equipment to ensure that surges in demand for healthcare can be adequately addressed; (2) long-term adequate reserves of material supplies to ensure the rapid setup of underground emergency hospitals [33]; (3) modular isolation equipment to ensure rapid start-up of URCs. Based on the above, the start-up conditions for epidemic-URCs require a joint progressive approach with local designated hospitals. The joint approach involves the following steps: designated hospitals receive patients; when the demand for healthcare in the designated hospitals increases significantly, epidemic-URCs are prepared in advance; when the healthcare capacity of the designated hospitals approaches saturation and the epidemic remains unsuppressed, epidemic-URCs are activated quickly. Timely activation of the centralized isolation of epidemic-URCs can effectively suppress outbreaks [34].

3.2. Disaster-URC

Urban multidisaster URCs were planned based on the Stock–Increment–Variable planning. Epidemic-URCs (Stock + Increment), disaster-URCs $(\text{Stock})_1$, and other multidisaster resilience $(\text{Stock})_n$ URCs were integrated. In contrast to the other multidisaster resilience URCs, megaseism-URCs have the following unique characteristics: (1) earthquakes are difficult to predict and last for a small duration; other disasters are predictable and the corresponding URCs can be prepared in advance and activated immediately. Therefore, epidemic resilience is the most challenging for URCs. (2) The shape and size of epidemic-URCs are significantly affected by the structural and geotechnical seismic vulnerabilities. The URCs for other disasters are not affected by the above factors but are related to the isolation from disasters by underground space. Therefore, disaster-URCs are dependent on the seismic vulnerability of underground structures and geotechnical environments, whereas other URCs are dependent on isolated and stable underground spaces. Therefore, megaseism disaster was analyzed for constructing the disaster-URC.

3.2.1. Finite Element Analysis Model and Parameters

Megaseism-FEA was performed for disaster-URC planning. Typical large underground space finite element models were established. Megaseism-FEA was performed to analyze the layout and efficiency of the disaster-URC. Thus, the Stock in large underground spaces and the layout of disaster-URCs were finally determined based on the megaseism-FEA results.

A 3D underground structural geotechnical coupling finite element model was built, and ADINA was used for megaseism-FEA. Based on the typical building and structural layout of the large underground space, the finite element models of Cross, T, and Block schemes were constructed (Figure 2a). The underground structure schemes were a typical five-floor multipan frame. The total height and longitudinal length are 28.5 and 240 m, respectively. Primarily, the dynamic response of structures was studied and the geotechnical models of typical underground structures were evaluated for earthquakes. Researchers have studied the seismic failure mechanism of the Daikai Station, which was severely damaged and collapsed in the 1995 Kobe earthquake [35,36]. Thus, data on the earthquake waves and geotechnical parameters of the Daikai Station earthquake were used [37]. Moreover, the Drucker–Prager material constitutive model was adopted for the input. The concrete model on ADINA based on nonlinear fracture mechanics was used for the concrete material constitutive model. A bilinear elastoplastic material constitutive model was used for steel. A geotechnical simulation was performed using eight-node 3D solid elements. The structural walls and plates were simulated with a four-node shell element. Reinforced concrete elements were simulated by integrating the concrete with equivalent reinforcement elements. An explicit dynamic analysis based on a large deformation displacement was conducted. The fracture condition was set as the maximum effective cumulative plastic strain. The elements were deleted to simulate damage and observe the structural damage location and modes.

A sophisticated 3D underground structure soil model with dimensions of 300 m $\times$ 1500 m $\times$ 150 m was established (Figure 2b). To ensure that the boundary had a negligible effect on the soil–structure interaction, the lateral boundary was more than five times the structure depth, and the bottom boundary was four times the structure height [16]. The bottom geotechnical elements were constrained by the freedom of the horizontal and vertical deformations. In the 3D soil–structure coupling model, the seismic deformations of the underground structure were constrained by the surrounding geotechnical elements. The following contacts were set at the interface between the structure and the soil elements: (a) the contact pressure was transferred when the interfaces were compressed; (b) tension was not transferred when the interfaces were separated; (c) the tangential deformation of the soil–structure interfaces were modeled by the Coulomb friction model with a friction coefficient of 0.4.

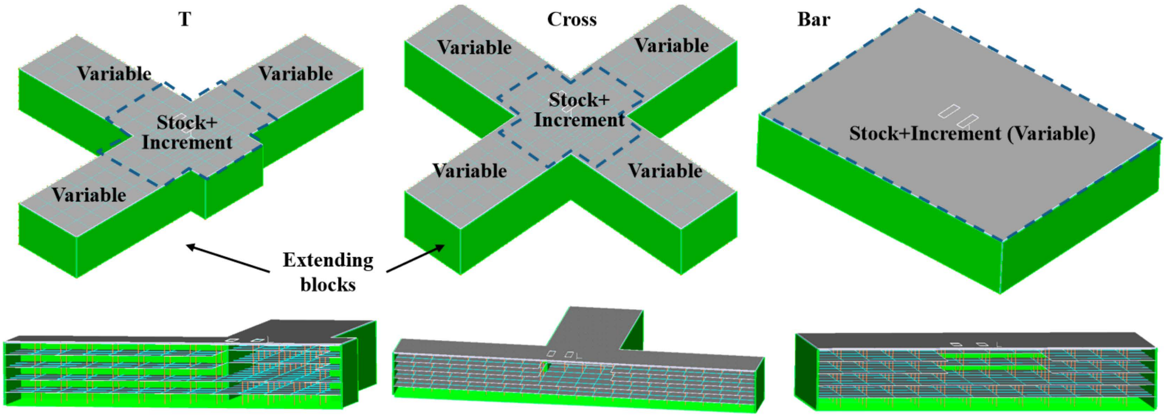

Structure component dimensions

Items	Roof thickness	Meddle plate thickness	Baseplate thickness	Exterial wall thickness	Columns	Roof beams	Meddle plate beams	Baseplate beams
Dimensions	1100/1200	600	1400	1000	○1500	1800×2000	1300×1600	2000×2600
Matetials	C35	C35	C35	C35	C50	C35	C35	C35

(**a**)

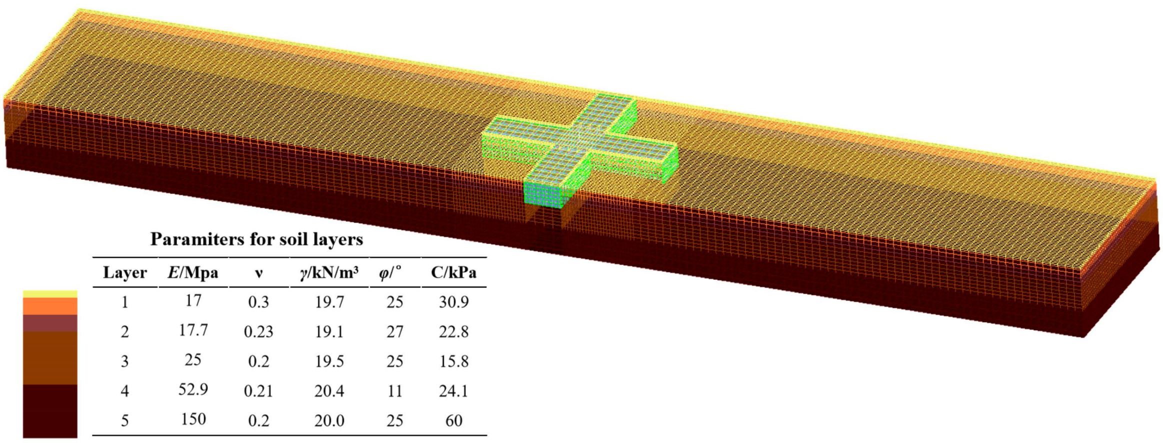

Paramiters for soil layers

Layer	*E*/Mpa	ν	γ/kN/m³	φ/°	C/kPa
1	17	0.3	19.7	25	30.9
2	17.7	0.23	19.1	27	22.8
3	25	0.2	19.5	25	15.8
4	52.9	0.21	20.4	11	24.1
5	150	0.2	20.0	25	60

(**b**)

Figure 2. Finite element models of Cross, T, and Bar schemes. (**a**) Structure models of Cross, T, and Block schemes; (**b**) Soil–structure finite element model.

3.2.2. Underground Structures Seismic Damage Modes

Figure 3 shows the results of the megaseism-FEA. Figure 3a presents that the seismic resilience of underground spaces is closely related to the soil–structure interactions. The extension blocks of the Cross(T) shape produced irregular soil–structure interaction interfaces with concave–convex corners. From the soil–structure interaction stress vector diagram, soil was subjected to high stress at the interfaces of the irregular walls, especially at the concave–convex position of the extending blocks. In contrast, a regular Bar-shaped underground space mainly produced lateral deformation. The Bar shape did not produce a superior interface for soil–structure interaction. It acted more evenly on the side span and the peak stress was shown at the intersection of the corner spans.

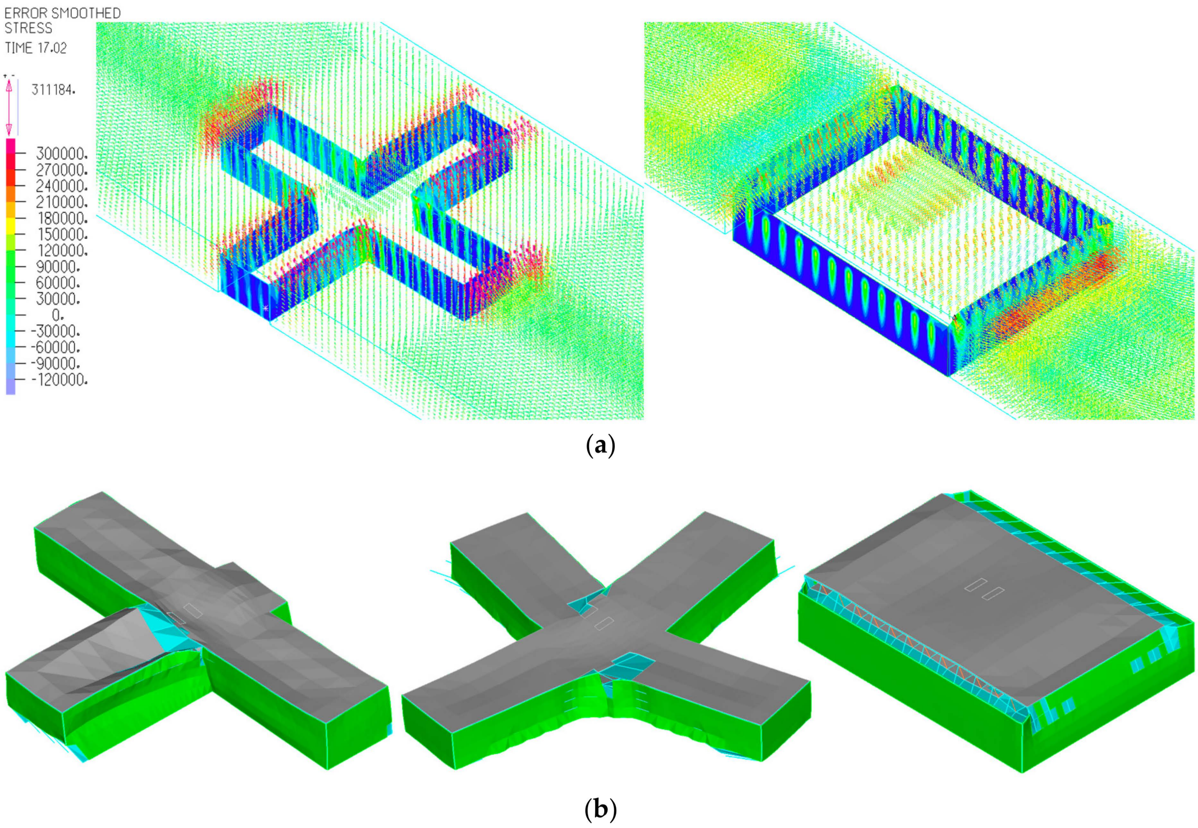

Figure 3. Results of megaseism-FEA for underground structures. (**a**) Soil–structure interaction stress vectors of Cross(T)-shaped and Bar-shaped schemes; (**b**) Damage modes of Cross, T, and Bar schemes.

Figure 3b shows the damage modes of the three megaseism-FEA schemes. The FEA failure was characterized as follows: (1) if the gray slab and green wall elements were deleted for reaching the fracture condition, and the blue reinforcement elements were exposed; (2) if the reinforcement elements were deleted, the region was considered completely collapsed. The damage mode of the Cross(T) shapes was torsional deformation. Under the action of megaseism, the extending blocks caused lateral deformation relative to the central URC area. Additionally, the soil–structure interaction intensified the soil pressure in the surrounding concave corners of the URC, making the area extremely vulnerable to damage. In contrast, the damage mode of the Bar shape was primarily lateral deformation due to the structural regularity and uniformity of the soil–structure interaction. The side span roof was finally destroyed by lateral deformation. Figure 4a,b show the time–history tensile stress of the walls and roofs of the Cross(T) shape. The interruption in the stress–time curve indicates that an element is damaged and removed. The first breakage occurred in the wall and roof elements at the concave–convex corners. The greater the tensile stress closer to the breaking point, the farther the element beyond the span of the column that remains intact.

In conclusion, the damage modes of the Cross, T, and Bar schemes determine the layout and size of the Stock and the URC. For the Cross(T) shape, the surrounding concave–convex walls of the URC and roofs fractured first. Subsequently, the cracks caused partial damage. Finally, the crack penetration caused the URC roof to become unconstrained and collapse, resulting in an instant 1/50 downward deflection (Figure 4c,d). Additionally, significant damage to the roof may cause serious secondary disasters: roof debris falling into the interior causes major accidents, and large deformations cause damage to equipment, especially for the B1 level. Therefore, the failure of concave corners compressed the layout and area of the Stock. In contrast, damage in the Bar shape occurred only in the outer span and did not affect the URC region. Therefore, the Bar shape has a larger area than the regular Stock.

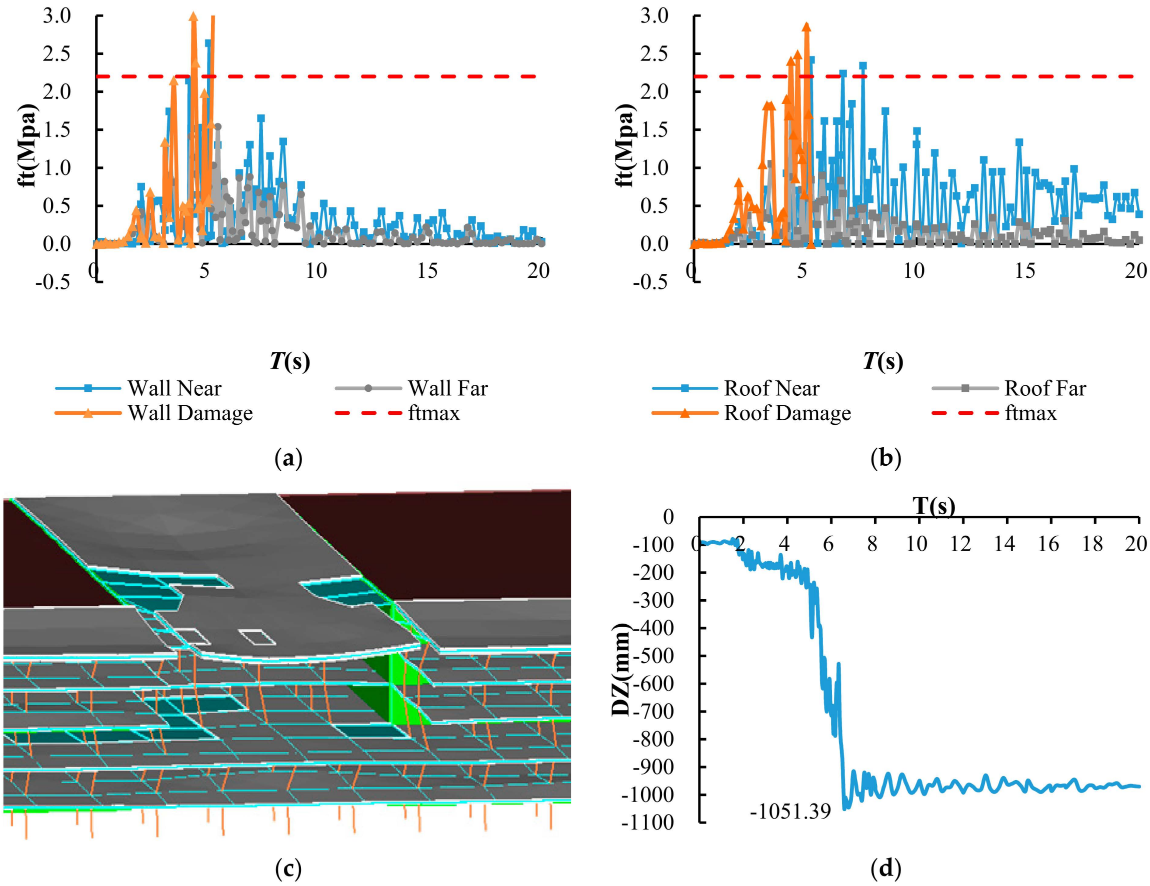

Figure 4. Cross(T)-shape time-history curves. (**a**) Tensile stress of Wall (**b**) Tensile stress of Slab; (**c**) URC roof collapses (**d**) Roof deformation.

3.3. Comprehensive-URC

The disaster analysis suggests that the comprehensive-URC can be planned through epidemic-URC and disaster-URC integration. First, according to Section 2.2, the damage mode was selected to build the Stock and the disaster-URC by determining a safe distance. According to Figure 4a,b, the elements that were one span away from the breakage remained intact. Therefore, the safe distance was defined as one span. Second, the Cross(T)-shaped Stock should not be considered for the B1 floor to ensure that the large roof deformations and falling objects can not affect the URC resilience. Finally, the Stock, disaster-URC, and comprehensive-URC were constructed for the Cross, T, and Bar underground spaces. The disaster-URC morphology derivation and Stock–Increment–Variable planning were shown in Figure 5.

Owing to the integration effect of the URCs, the URCs exhibit organized and hierarchical characteristics. The integration effect of epidemic- and disaster-URCs presented the following effects: (1) the emergency resources and capabilities in the underground space were concentrated in the Stock. Thus, the Stock formed a robust urban space. (2) Increment of the underground space was prepared for rapid and flexible transformation. The Stock can immediately activate the peripheral Increment for resilient reinforcement to cope with multidisaster uncertainty. Thus, Increment represented a redundant and resourceful space. (3) Variable was developed in an underground space that can be renovated and upgraded. In the future, Variable can be renovated into the Stock or Increment on demand to respond intelligently to multidisaster situations in cities.

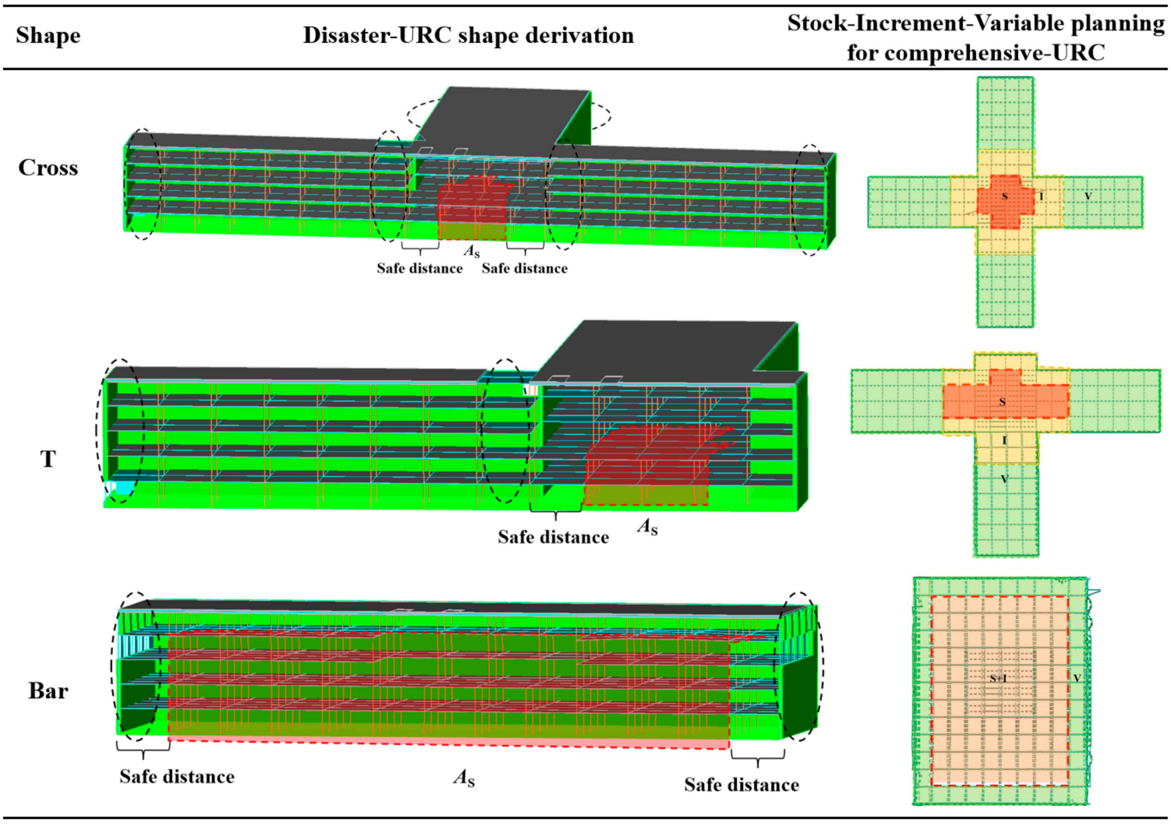

Figure 5. Comparison of URC planning.

4. URC Assessment Results

A morphology and resilience assessment of the URC schemes was conducted, and the optimum comprehensive resilience scheme was obtained.

4.1. URC Morphology Assessment Results

Disaster-based Stock–Increment–Variable planning reveals the efficiency of the URCs for different large underground spaces (Figure 6a). For the Stock, the regular Bar shape damage mode had a limited impact on the URC; thus, 68% of the disaster resilience space was obtained. In contrast, the Cross and T damage modes constrained the URC layout, owing to the exclusion of the B1 level, which significantly reduced the URC area. Consequently, the disaster resilience spaces of the Cross and T shapes were only 20.59% and 30.88% of that of the Bar shape, respectively. Further, for the Stock + Increment, the Bar-shaped underground space enabled the large space for Stock–Increment–Variable transformation; thus, a larger epidemic management space was obtained. The functions of Cross(T)-shaped underground hubs were generally more complex, and the distribution of flexible large spaces was compact and concentrated. Moreover, the T shape was one extending block less than the Cross shape for epidemic management. The epidemic resilience spaces of the Cross and T shapes were 0.83 and 0.73 times that of the Bar shape, respectively. In general, comprehensive resilience adopts the integration of epidemic–disaster management. The URC planning efficiency of underground space in different scenarios is ranked as follows: the Bar shape leads overall, the T shape leads second for disaster resilience, and the Cross shape leads second for epidemic resilience.

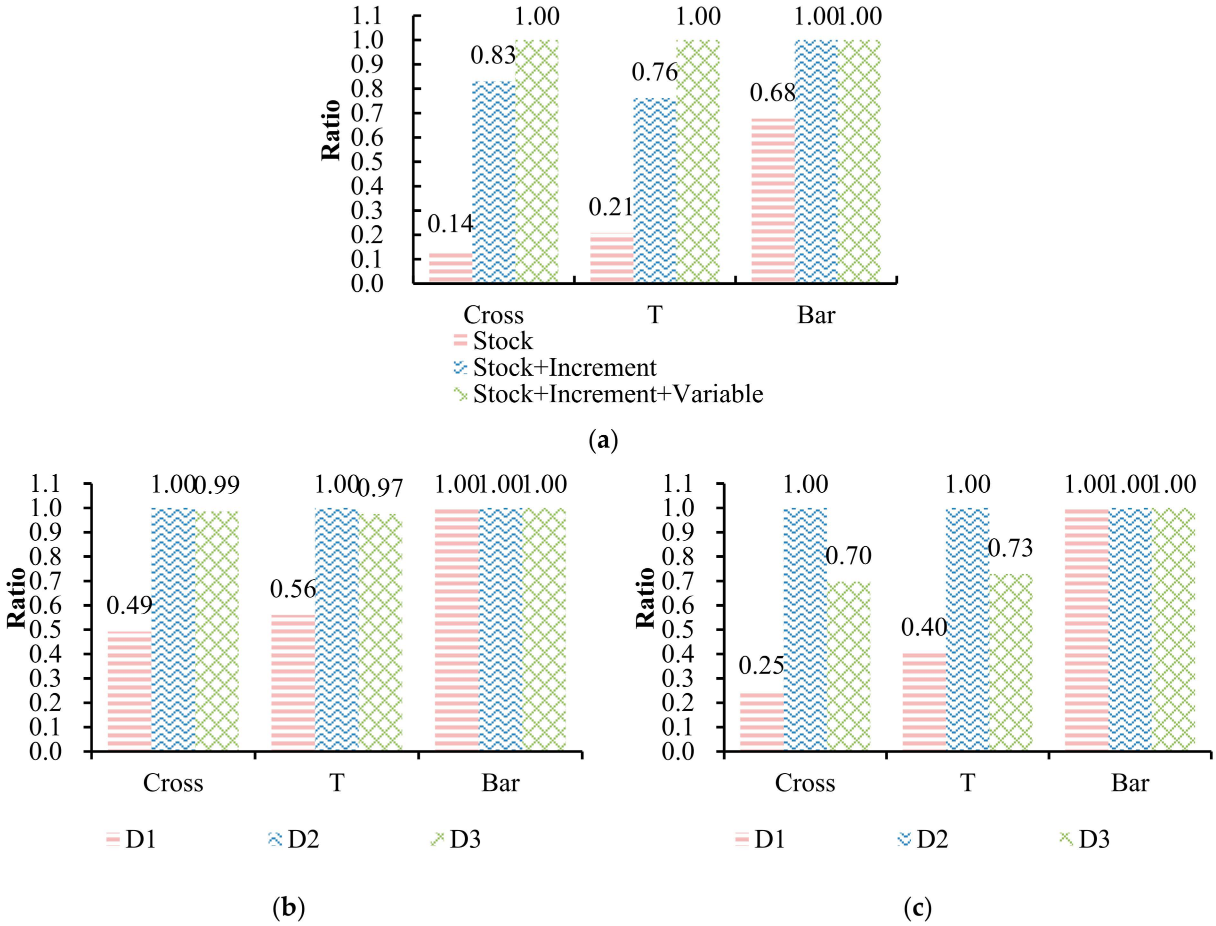

Figure 6. URC planning and morphology assessment. (**a**) Disaster-based URC planning; (**b**) Epidemic-URC morphology assessment (**c**) Disaster-URC morphology assessment.

The URC morphology indicators (Equations (1)–(3)) quantified the URC efficiency (Figure 6b,c). The evaluation results were standardized using the D1 indicators. Considering the epidemic-URCs, the most significant difference among the URC morphology indicators was the D1 indicator. This indicates that the Cross(T) shape, which can only be developed in the central region, is not as efficient as the Bar shape. Regarding disaster-URCs, D1 increased with increasing D3, indicating that the more regular the underground space morphology, the larger the URC area. Furthermore, for the megaseism-FEA, structural irregularities increased the adverse effects of soil on the Cross(T) shape and torsional damage mode. Therefore, both the megaseism-FEA and URC morphology indicators demonstrate that the regularity of underground space determined the seismic performance, shape, and size of the URC because there was no URC dispersion in any of the three schemes, and D2 is 1. In general, URC morphology indicators are consistent with the epidemic–disaster analysis results and accurately reflect the URC efficiency of large underground spaces.

4.2. Comprehensive Resilience Assessment Results

Based on the above analysis, the comprehensive resilience of URCs in typical large underground spaces can be evaluated. Two urban emergency scenarios were established using the time–history data of the COVID-19 in Wuhan and Kobe earthquakes. The original scenario employing a large number of temporary isolation hospitals served as the basic data [38]. The effect of activating individual URCs, in combination with the original scenario, on urban resilience was analyzed. Data from the original scenario and activation of only designated hospitals were used as the two comparative scenarios. According to

Section 2.2.2, $Q_c - T$, $Q_{Bar} - T$, and R functions were used for the comprehensive resilience assessment (Figure 7).

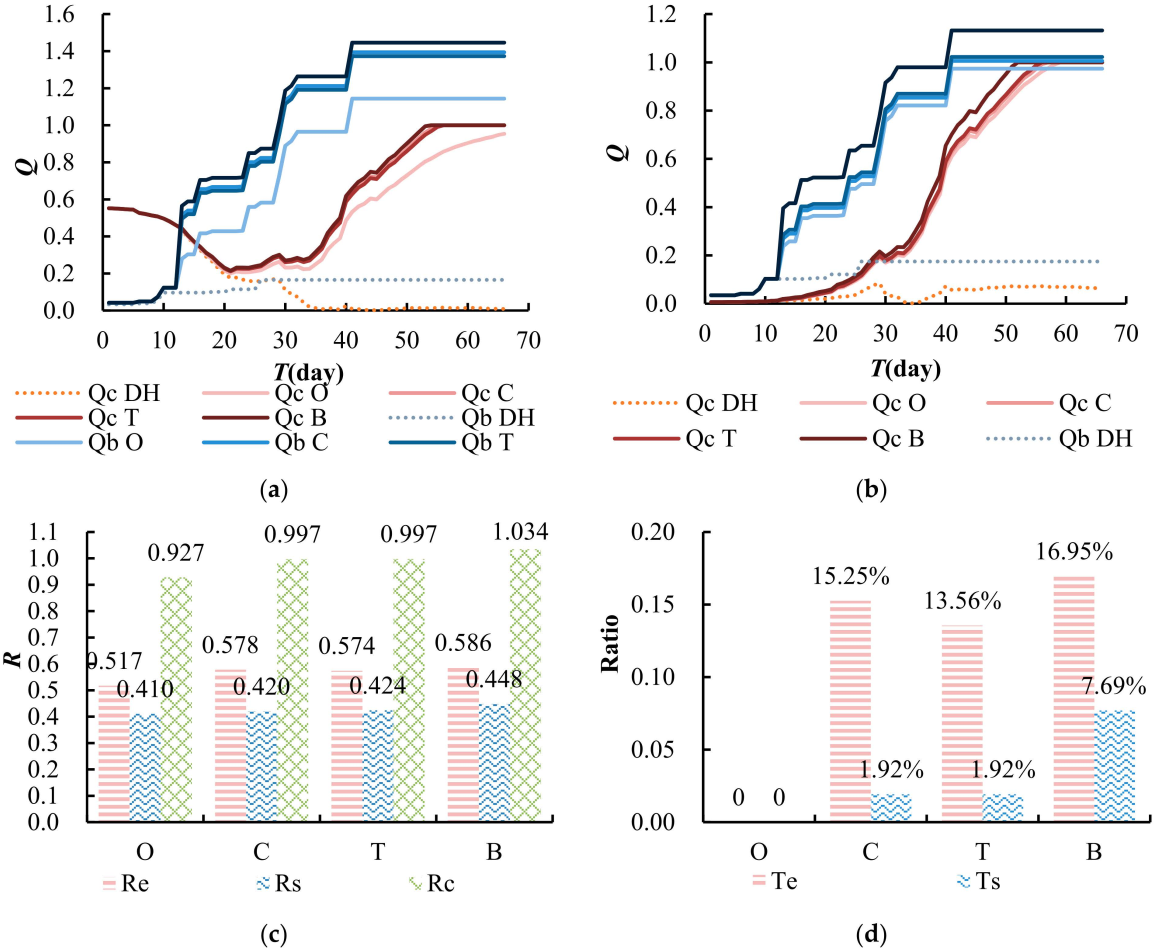

Figure 7. $Q - T$ and comprehensive resilience assessments for designated hospitals and Cross-/T-/Bar-shaped URCs. (**a**) Epidemic $Q - T$ (**b**) Disaster $Q - T$; (**c**) Resilience R assessment (**d**) Recovery time T assessment. Note: DH, O, C, T, and B indicate only activating designated hospitals, the original scenario of activating temporary isolation hospitals, and Cross-/T-/Bar-shaped URCs with this, respectively. R_e, R_s, and R_c indicate the resilience functions for the epidemic, disaster, and comprehensive resilience, respectively (Equations (8) and (9)). T_e and T_s indicate the advanced recovery times for epidemics and disasters, respectively.

The $Q - T$ and R functions quantified the two scenarios for postdisaster recovery. In urban epidemic scenarios, the Stock + Increment of a URC can provide a substantial bed supply. The $Q_{Bar} - T$ curve showed that the urban epidemic resistance was significantly improved compared to the original scenario by utilizing URCs (Figure 7a). In the urban megaseism scenario, URCs activate the Stock to provide shelter beds, but the $Q_{Bar} - T$ curve indicates that only the Bar-shaped URCs lead to significant improvements (Figure 7b). Quantified by the R function, the contribution of a single URC to the epidemic resilience was from 11.03% to 13.35%, and that to the disaster resilience was from 2.44% to 9.27%. Consequently, the urban comprehensive resilience was improved after the provision of additional bed supplies by the three schemes. For the comprehensive resilience, the Bar-shaped URC with an 11.54% R_c improvement led to a significant advantage (Figure 7c). The comprehensive resilience of the Cross- and T-shaped URCs was consistent (R_c = 0.997), while each had second place in disaster resilience and epidemic resilience, respectively.

The Q_c-T function represents the evolutionary trend of the urban epidemic–seismic asylum demands. Epidemic outbreaks are infectious and repetitive. Therefore, $Q_c - T$

exhibited a decreasing evolution in the period of day 20 to day 40. In contrast, a large number of asylum demands were generated instantaneously after a megaearquake, and the starting point of the $Q_c - T$ curve became the most vulnerable moment. A comparison of $Q_{Bar} - T$ and $Q_c - T$ curves elucidates the effect of bed supply on the recovery from urban epidemics and disasters. From Figure 7a,b, it can be inferred that, if only the designated hospitals were activated, cities cannot recover quickly in epidemic–seismic scenarios. In contrast, when Q_b increases to a supply–demand balance (Q_b = 1), the epidemic $Q_c - T$ curve showed a turning point and began to recover. Similarly, the disaster $Q_c - T$ showed a Gaussian curve feature and began to accelerate recovery at Q_b = 1; this indicates that adequate bed supply is a critical condition for urban comprehensive resilience. The recovery time was analyzed in Figure 7d and assumed that the Q_c recovery was 0.9. The recovery time of the Bar-shaped URC under the two scenarios reached the target by 16.95% and 7.69% earlier, demonstrating an excellent recovery capability. Cross- and T-shaped URCs contributed significantly (15.25% and 13.56%, respectively) to the advanced recovery time under epidemic scenarios. However, their contribution (1.92%) to the advanced recovery time under disaster was negligible.

5. Potential Analysis for Comprehensive Resilience of Urban Underground Space in China

The above analysis indicates that URC planning in underground spaces can improve the current urban comprehensive resilience significantly. Among the underground structures considered, underground parking has a regular shape and flexible layout and is common in urban residential, commercial, and public buildings. The development of urban underground parking areas in URCs has great potential for comprehensive epidemic–disaster management. Therefore, the comprehensive resilience of urban underground parking areas was assessed for URC planning in China. The "Blue Book on Urban Underground Space Development in China 2021" was used to select 100 sample cities for statistics based on the economic profile, social basis, and traffic demand [39]. Thus, data on the cities was used to obtain the urban underground parking area data with sample characteristics and reliable data sources (Figure 8a). The number of people affected by the COVID-19 epidemic in Wuhan [28] and the Kobe earthquakes [29] were also used as data. The total underground parking area corresponding to the affected people was calculated based on 35 m^2/car using the Chinese "Design Code for Garage" [40]. Additionally, underground parking is presented as a large, Bar-shaped underground space. Based on the Stock–Increment–Variable planning of the Bar-shaped URC in Figure 6a, the data from Figure 8a were converted into data on epidemic- and disaster-URC areas of the sample cities and average data as Figure 8b.

Figure 9 shows the potential analysis for the comprehensive resilience of urban underground space in China. The data on Hangzhou and Wuhan ranked at the top and middle in the urban underground space development index in China. The data of these two cities and the average data were selected for comprehensive resilience assessment and demonstration (Figure 9). $Q_b - T$ curves showed that cities with medium or higher underground space development (Hangzhou, Wuhan) can provide more than 10 and 4 times the bed demand, respectively (Figure 9a,c). For epidemic–seismic management, the increase in the bed capacity can accommodate the need for treatment and shelter in urban epidemics and disasters. The $Q_c - T$ function assessed that the recovery time to Q_c = 0.9 was from 42% to 63% earlier, and the R_C function assessed that the comprehensive resilience was from 62.37% to 66.67% higher (Figure 9e,f). Therefore, Chinese cities with above medium underground parking development intensity have reserves for strong epidemic–seismic resilience.

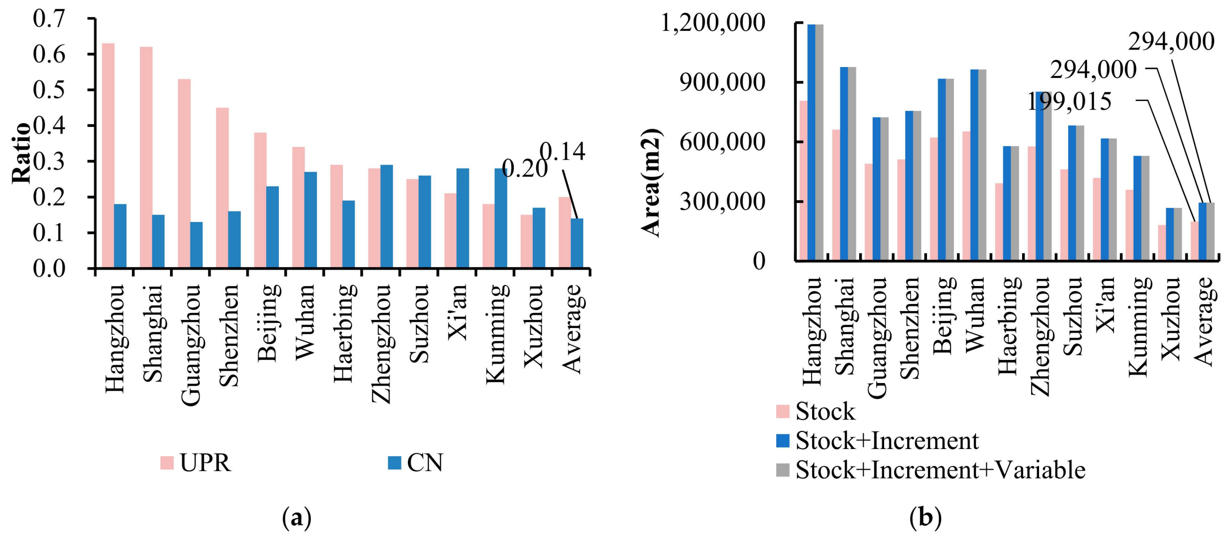

Figure 8. Stock–Increment–Variable planning for urban underground spaces in China. (**a**) Underground parking areas (**b**) Stock–Increment–Variable planning of cities' underground parking areas of cities. Note: UPR indicates underground parking ratio. CN indicates the number of cars/ people.

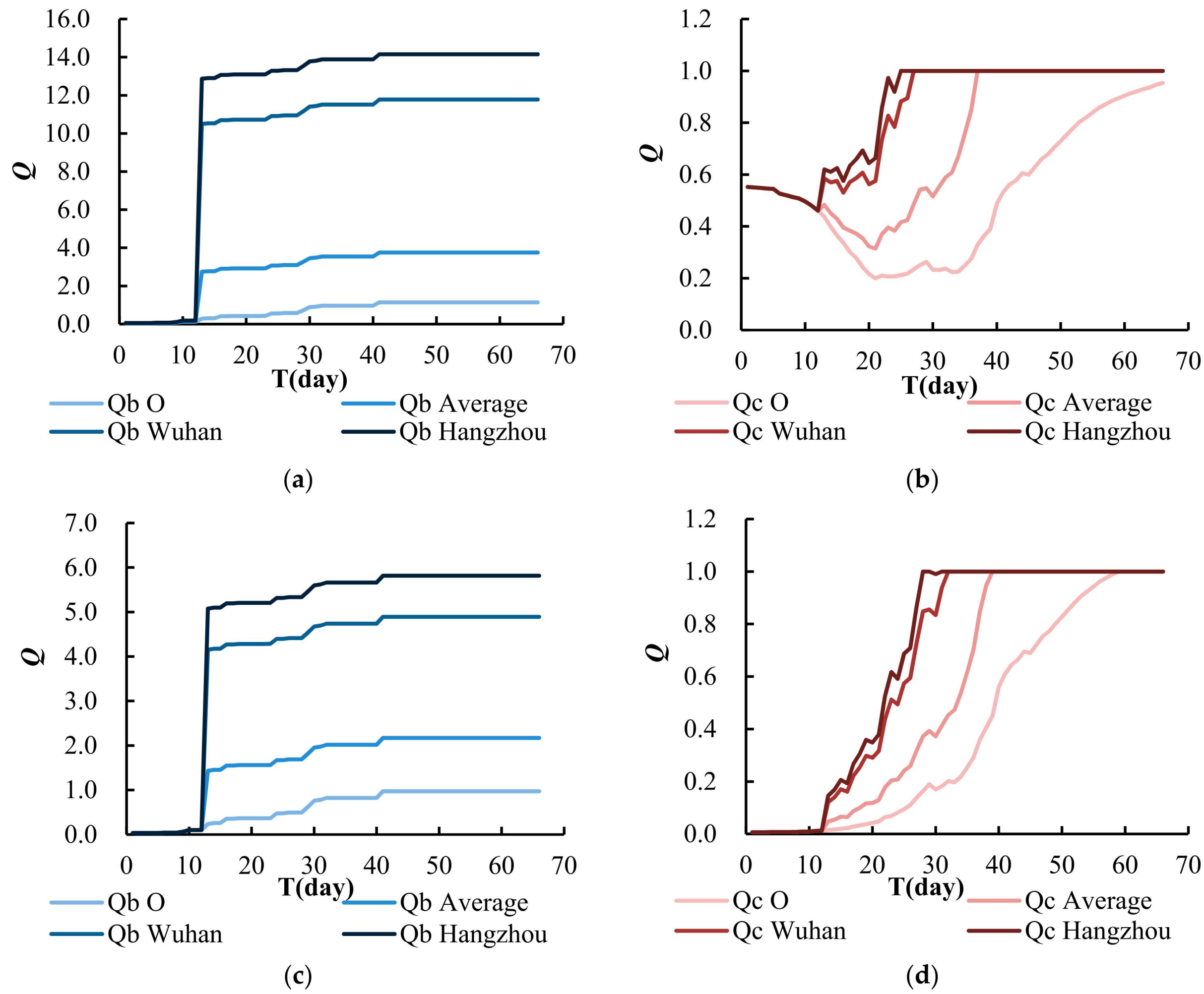

Figure 9. *Cont.*

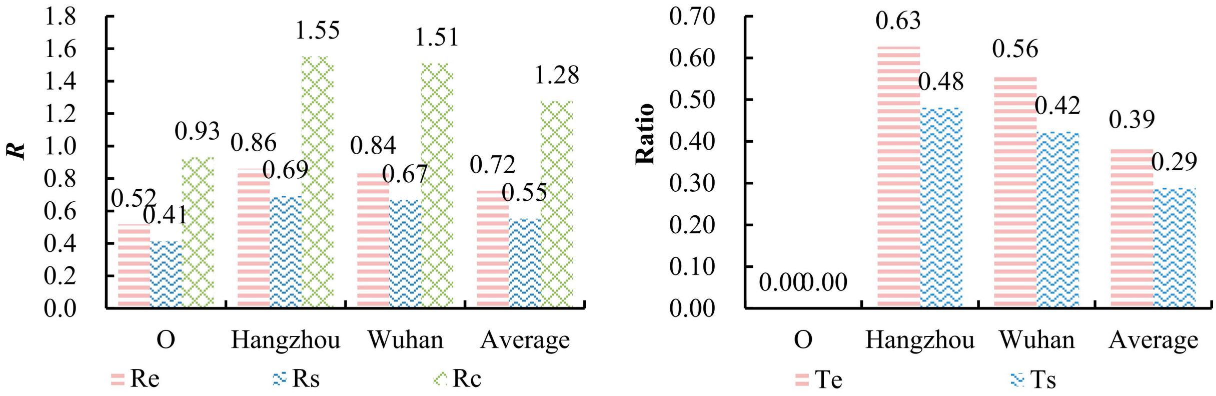

(e) (f)

Figure 9. Potential analysis for comprehensive resilience of urban underground space in China. (**a**) Epidemic Q_b; (**b**) Epidemic Q_c; (**c**) Disaster Q_b; (**d**) Disaster Q_c; (**e**) Comparison of *R*; (**f**) Comparison of *T*.

The average underground parking data can characterize the comprehensive resilience potential for epidemic–disaster management. Figure 9b showed the epidemic reversal from day 20 to day 40 for Wuhan, owing to insufficient bed supply (Q_c O). Figure 9a,c showed that URCs can quickly release 1.5 to 3 times the bed demand during epidemics and megaseisms using underground parking. In particular, URC planning for underground parking can cause the reversal trend of the epidemic to disappear (Figure 9b). The turning point of the $Q_c - T$ curve advanced from the original 35 day to 21 day. Additionally, the disaster $Q_c - T$ curve approximated the recovery pattern of the Gaussian curve under the original bed supply. If an average underground parking area was employed, the recovery of the $Q_c - T$ curve was significantly accelerated (near-linear recovery for the above medium cities) (Figure 9d). Therefore, superimposing the underground parking as URCs leads to a significant improvement in the urban epidemic–disaster recovery performance. Finally, the recovery time to reach Q_c = 0.9 was 29% to 39% earlier as assessed by the $Q_c - T$ function, and the comprehensive resilience was 37.63% higher as assessed by the R_C function. In summary, if underground parking in China is fully developed for URC planning, it possesses significant potential to improve urban comprehensive resilience.

6. Discussion

In response to the proposed strategies and assessment results, this study discusses the following:

1. Adequate shelter space accelerates resilience recovery from epidemics and disasters. Especially for epidemics, sufficient bed supply anticipates the emergence of performance turning points and avoids the recurrence of epidemics. This reveals that adequate space planning is necessary to enhance comprehensive urban resilience. The current use of aboveground space for disaster management remains challenging, owing to the special requirements of the epidemic–disaster management space. The results of the assessment indicate that the current use of only aboveground designated hospitals is not sufficient to respond to disaster outbreaks and is not conducive to long-term epidemic–disaster resilience management.
2. The assessment results suggest that the use of existing urban underground space in China can significantly enhance the comprehensive resilience of the city. Unlike some studies that used new construction to improve urban resilience [41,42], this study advocates the use of existing urban space to improve urban resilience. URC planning is the utilization of three modules as Stock, Increment, and Variable within the underground space. This strategy does not require new large-scale civil construction, but only the utilization of underground spaces. URC planning reflects the refined

management of underground resources [43,44] and exploits the potential of urban underground space.

3. The URC planning and assessment method have adaptability for long-term urban disaster management. For cities that have built certain underground spaces, URC planning can be initiated immediately to enhance the comprehensive resilience at the earliest. For cities that have not built sufficient underground spaces, the proposed resilience assessment method can be used to assess the current resilience state. This will produce the following results: if aboveground space is sufficient for resilience construction (designed hospitals) and does not interfere with urban functions, there is no need to use underground space for epidemic control; if both aboveground space and underground space do not meet epidemic resilience demands, the resilience assessment gives quantitative results. The poor resilience assessment result is exactly what urban construction should focus on. This provides an important reference value for developing the future resilience construction of cities. Therefore, the strategy and assessment method of URC planning can both adapt to the existing underground space to enhance urban resilience and provide an important reference for the future resilience construction of the cities.

7. Conclusions

In this study, the planning and assessment of URCs were investigated. Epidemic- and disaster-URCs were planned in typical large underground spaces. Subsequently, the epidemic- and disaster-URCs were integrated to construct comprehensive-URCs. Finally, the comprehensive resilience potential of urban underground spaces in China was analyzed. The results of this study were summarized as follows:

1. The efficiency of epidemic-URCs depends on its area, whereas disaster-URCs also require consideration of morphology. Underground space use large flexible spaces for planning epidemic-URCs. The megaseism damage modes determine the layout and size of the disaster-URC.
2. Morphology of underground spaces is essential for comprehensive resilience. The URC morphology indicators reveal that the more regular the morphology, the larger the URC area. Irregular Cross(T)-shaped disaster-URCs are subject to considerable constraints. URC planning efficiency is ranked as follows: the Bar shape leads overall, the T shape leads second under disaster resilience, and the Cross shape leads second under epidemic resilience.
3. The epidemic–seismic scenario assessment shows that bed supply comparable to bed demand is the key for recovery. In this case, the epidemic-cured performance presents a turning point, whereas the disaster-cured performance shows rapid recovery. An individual Bar-shaped URC can improve comprehensive resilience by 11.54% over the current application of upper temporary isolated hospitals. Cross(T)-shaped URCs contribute significantly to the epidemic scenario (15.25% and 13.56%); however, their contribution is low in the case of disasters (1.92%).
4. Chinese cities with above-medium-intensity underground parking development have potential for strong resilience to epidemics and disasters. If the Chinese underground parking resources are efficiently utilized for URC planning, the recovery time will be 29% to 39% earlier, and the comprehensive resilience will be improved by 37.63%.

The present research results have practical value for urban long-term comprehensive epidemic–disaster management and URC planning in urban underground spaces.

Author Contributions: Conceptualization, T.Q.; methodology, T.Q.; software, T.Q. and X.L.; validation, T.Q.; formal analysis, T.Q.; investigation, T.Q.; resources, T.Q.; data curation, T.Q. and X.L.; writing—original draft preparation, T.Q.; writing—review and editing, D.S.; visualization, T.Q.; supervision, D.S.; project administration, X.C.; funding acquisition, X.C. All authors have read and agreed to the published version of the manuscript.

Funding: This research was funded by the National Natural Science Foundation of China (NSFC) (project number: 51938008).

Data Availability Statement: Not applicable.

Conflicts of Interest: The authors declare no conflict of interest.

References

1. Cuadros, D.F.; Branscum, A.J.; Mukandavire, Z.; Miller, F.D.; MacKinnon, N. Dynamics of the COVID-19 epidemic in urban and rural areas in the United States. *Ann. Epidemiol.* **2021**, *59*, 16–20. [CrossRef] [PubMed]
2. Barua, U.; Islam, I.; Ahmed Ansary, M. Integration of earthquake risk- sensitivity into landuse planning: An approach for a local level area at development phase. *Int. J. Disaster Risk Reduct.* **2020**, *50*, 101836. [CrossRef]
3. Liang, L.; Wang, Z.; Li, J. The effect of urbanization on environmental pollution in rapidly developing urban agglomerations. *J. Clean. Prod.* **2019**, *237*, 117649. [CrossRef]
4. Simić, V.; Ivanović, I.; Đorić, V.; Torkayesh, A.E. Adapting Urban Transport Planning to the COVID-19 Pandemic: An Integrated Fermatean Fuzzy Model. *Sustain. Cities Soc.* **2022**, *79*, 103669. [CrossRef]
5. Liu, S.-C.; Peng, F.-L.; Qiao, Y.-K.; Zhang, J.-B. Evaluating disaster prevention benefits of underground space from the perspective of urban resilience. *Int. J. Disaster Risk Reduct.* **2021**, *58*, 102206. [CrossRef]
6. Zhang, W.; Shi, X.; Huang, A.; Hua, G.; Teunter, R.H. Optimal stock and capital reserve policies for emergency medical supplies against epidemic outbreaks. *Eur. J. Oper. Res.* **2021**, *304*, 183–191. [CrossRef]
7. Xie, H.; Zhang, Y.; Chen, Y.; Peng, Q.; Liao, Z.; Zhu, J. A case study of development and utilization of urban underground space in Shenzhen and the Guangdong-Hong Kong-Macao Greater Bay Area. *Tunn. Undergr. Space Technol.* **2021**, *107*, 103651. [CrossRef]
8. Chen, Y.; Lei, J.; Li, J.; Zhang, Z.; Yu, Z.; Du, C. Design characteristics on the indoor and outdoor air environments of the COVID-19 emergency hospital. *J. Build. Eng.* **2022**, *45*, 103246. [CrossRef]
9. Haike_News. Shanghai Was Hit by the Storm, Temporary Hospitals Severe Leakage, Staff Rescue Overnight. 2022. Available online: https://haokan.baidu.com/v?vid=15625277830104091464 (accessed on 14 April 2022).
10. Zhang, Y.; Zhu, J.; Liao, Z.; Guo, J.; Xie, H.; Peng, Q. An intelligent planning model for the development and utilization of urban underground space with an application to the Luohu District in Shenzhen. *Tunn. Undergr. Space Technol.* **2021**, *112*, 103933. [CrossRef]
11. Bar-El, Y.; Reisner, S.; Beyar, R. Moral dilemmas faced by hospitals in time of war: The Rambam Medical Center during the Second Lebanon War. *Med. Health Care Philos.* **2013**, *17*, 155–160. [CrossRef]
12. Haverkort, J.M.; de Jong, M.B.; Foco, M.; Gui, D.; Barhoum, M.; Hyams, G.; Bahouth, H.; Halberthal, M.; Leenen, L.P. Dedicated mass-casualty incident hospitals: An overview. *Injury* **2017**, *48*, 322–326. [CrossRef]
13. Yu, Y.; You, S.; Zhang, H.; Ye, T.; Wang, Y.; Wei, S. A review on available energy saving strategies for heating, ventilation and air conditioning in underground metro stations. *Renew. Sustain. Energy Rev.* **2021**, *141*, 110788. [CrossRef]
14. Hu, W.; Dong, J.; Hwang, B.-G.; Ren, R.; Chen, Z. A preliminary prototyping approach for emerging metro-based underground logistics systems: Operation mechanism and facility layout. *Int. J. Prod. Res.* **2021**, *59*, 7516–7536. [CrossRef]
15. Xu, Y.; Dong, J.; Ren, R.; Yang, K.; Chen, Z. The impact of metro-based underground logistics system on city logistics performance under COVID-19 epidemic: A case study of Wuhan, China. *Transp. Policy* **2022**, *116*, 81–95. [CrossRef] [PubMed]
16. Li, W.; Chen, Q. Seismic damage evaluation of an entire underground subway system in dense urban areas by 3D FE simulation. *Tunn. Undergr. Space Technol.* **2020**, *99*, 103351. [CrossRef]
17. Tsinidis, G. Response characteristics of rectangular tunnels in soft soil subjected to transversal ground shaking. *Tunn. Undergr. Space Technol.* **2017**, *62*, 1–22. [CrossRef]
18. Sayed, M.A.; Kwon, O.-S.; Park, D.; Van Nguyen, Q. Multi-platform soil-structure interaction simulation of Daikai subway tunnel during the 1995 Kobe earthquake. *Soil Dyn. Earthq. Eng.* **2019**, *125*, 105643. [CrossRef]
19. Dong, R.; Jing, L.; Li, Y.; Yin, Z.; Wang, G.; Xu, K. Seismic deformation mode transformation of rectangular underground structure caused by component failure. *Tunn. Undergr. Space Technol.* **2020**, *98*, 103298. [CrossRef]
20. Zhong, Z.; Shen, Y.; Zhao, M.; Li, L.; Du, X.; Hao, H. Seismic fragility assessment of the Daikai subway station in layered soil. *Soil Dyn. Earthq. Eng.* **2020**, *132*, 106044. [CrossRef]
21. Zhang, W.; Yun, Y. Multi-scale accessibility performance of shelters types with diversity layout in coastal port cities: A case study in Nagoya City, Japan. *Habitat Int.* **2019**, *83*, 55–64. [CrossRef]
22. Alam, E. Importance of long-term earthquake, tsunami and tropical cyclone data for disaster risk reduction in Bangladesh. *Prog. Disaster Sci.* **2019**, *2*, 100019. [CrossRef]
23. Li, H.; Zhao, L.; Huang, R.; Hu, Q. Hierarchical earthquake shelter planning in urban areas: A case for Shanghai in China. *Int. J. Disaster Risk Reduct.* **2017**, *22*, 431–446. [CrossRef]
24. Breçani, R.; Dervishi, S. Thermal and energy performance evaluation of underground bunkers: An adaptive reuse approach. *Sustain. Cities Soc.* **2019**, *46*, 101444. [CrossRef]
25. Kitamura, F.; Inazu, D.; Ikeya, T.; Okayasu, A. An allocating method of tsunami evacuation routes and refuges for minimizing expected casualties. *Int. J. Disaster Risk Reduct.* **2020**, *45*, 101519. [CrossRef]

26. Ćurković, M.; Svetina, L.; Košec, A. Double jeopardy; What happens when an epidemic is followed by an earthquake? *Spat. Spatio-Temporal Epidemiol.* **2021**, *36*, 100402. [CrossRef] [PubMed]
27. Xu, J.; Yin, X.; Chen, D.; An, J.; Nie, G. Multi-criteria location model of earthquake evacuation shelters to aid in urban planning. *Int. J. Disaster Risk Reduct.* **2016**, *20*, 51–62. [CrossRef]
28. Xu, G.; Jiang, Y.; Wang, S.; Qin, K.; Ding, J.; Liu, Y.; Lu, B. Spatial disparities of self-reported COVID-19 cases and influencing factors in Wuhan, China. *Sustain. Cities Soc.* **2022**, *76*, 103485. [CrossRef]
29. Sogabe, T.; Maki, N. Do disasters provide an opportunity for regional development and change the societal trend of impacted communities?: Case study on the 1995 Kobe earthquake. *Int. J. Disaster Risk Reduct.* **2022**, *67*, 102648. [CrossRef]
30. Henry, D.; Ramirez-Marquez, J.E. Generic metrics and quantitative approaches for system resilience as a function of time. *Reliab. Eng. Syst. Saf.* **2012**, *99*, 114–122. [CrossRef]
31. Haiyang; Ziyang, F. The Shelter Hospital of Wuhan Hongshan Gymnasium will Build “Three Areas and Two Channels” to Avoid Cross Infection. *BJNEWS* **2020**. Available online: https://baijiahao.baidu.com/s?id=1657651008571928756&wfr=spider&for=pc (accessed on 5 February 2020).
32. Gbadamosi, A.-Q.; Oyedele, L.; Olawale, O.; Abioye, S. Offsite Construction for Emergencies: A focus on Isolation Space Creation (ISC) measures for the COVID-19 pandemic. *Prog. Disaster Sci.* **2020**, *8*, 100130. [CrossRef]
33. Zhang, T.; Wang, Q.; Leng, Z.; Yang, Y.; Yang, J.; Chen, F.; Jia, M.; Zhang, X.; Qi, W.; Xu, Y.; et al. A Scenario-Based Evaluation of COVID-19-Related Essential Clinical Resource Demands in China. *Engineering* **2021**, *7*, 948–957. [CrossRef]
34. Bhadoria, A.S.; Gawande, K.; Sharma, R.; Mohapatra, A.; Kant, R. Institutional versus home isolation to curb the COVID-19 outbreak. *Lancet* **2020**, *396*, 1631–1632. [CrossRef]
35. An, X.; Shawky, A.A.; Maekawaa, K. The collapse mechanism of a subway station during the Great Hanshin earthquake. *Cem. Concr. Compos.* **1997**, *19*, 241–257. [CrossRef]
36. Lu, C.-C.; Hwang, J.-H. Nonlinear collapse simulation of Daikai Subway in the 1995 Kobe earthquake: Necessity of dynamic analysis for a shallow tunnel. *Tunn. Undergr. Space Technol.* **2019**, *87*, 78–90. [CrossRef]
37. Sandoval, E.; Bobet, A. The undrained seismic response of the Daikai Station. *Tunn. Undergr. Space Technol.* **2020**, *103*, 103474. [CrossRef]
38. Pengpai_News. *How Many Beds Are There in Wuhan to Deal with COVID-19 Epidemic?* Pengpai News: Wuhan, China, 2020. Available online: https://baijiahao.baidu.com/s?id=1658385426681451867&wfr=spider&for=pc (accessed on 13 February 2020).
39. Zhilong, C.; Dong, J. 2021 Blue Book on Urban Underground Space Development in China. 2021. Available online: http://www.csrme.com/Home/Content/show/id/3034.do (accessed on 28 December 2021).
40. BUCEA. *Design Code for Garage*; Ministry of Housing and Urban Rural Development of the People’s Republic of China: Beijing, China, 1998.
41. Ro, B.; Garfin, G. Building urban flood resilience through institutional adaptive capacity: A case study of Seoul, South Korea. *Int. J. Disaster Risk Reduct.* **2023**, *85*, 103474. [CrossRef]
42. Taheri, B.; Molzahn, D.K.; Grijalva, S. Improving distribution system resilience by undergrounding lines and deploying mobile generators. *Electr. Power Syst. Res.* **2023**, *214*, 108804. [CrossRef]
43. Luo, L.; Xu, L.; Shi, X.; Meng, J.; Liu, R. Microscale insights into the influence of grinding media on spodumene micro-flotation using mixed anionic/cationic collectors. *Int. J. Min. Sci. Technol.* **2022**, *32*, 171–179. [CrossRef]
44. Wang, S.; Xia, Q.; Xu, F. Investigation of collector mixtures on the flotation dynamics of low-rank coal. *Fuel* **2022**, *327*, 125171. [CrossRef]